

The 14th International Topical Meeting on Nuclear Reactor Thermal Hydraulics, NURETH-14
Toronto, Ontario, Canada, September 25-30, 2011

NURETH14-153

**ASSESSMENT OF CTF BOILING TRANSITION AND CRITICAL HEAT FLUX
MODELING CAPABILITIES USING THE OECD/NRC BFBT AND PSBT BENCHMARK
DATABASES**

Maria Avramova¹ and Diana Cuervo²

¹The Pennsylvania State University, University Park, PA, USA

²Department of Nuclear Engineering, Technical University of Madrid, Madrid, Spain

mna109@psu.edu and d.cuervo@upm.es

Abstract

The need to refine models for best-estimate calculations, based on good-quality experimental data, has been expressed in many recent meetings in the field of nuclear applications. The modeling needs arising in this respect should not be limited to the currently available macroscopic methods but should be extended to next-generation analysis techniques that focus on more microscopic processes. One of the most valuable databases identified for the thermal-hydraulics modeling was developed by the Nuclear Power Engineering Corporation (NUPEC), Japan. From 1987 to 1995, NUPEC performed steady-state and transient critical power and departure from nucleate boiling (DNB) test series based on the equivalent full-size mock-ups. Considering the reliability not only of the measured data, but also other relevant parameters such as the system pressure, inlet sub-cooling and rod surface temperature, these test series supplied the first substantial database for the development of truly mechanistic and consistent models for boiling transition and critical heat flux.

Over the last few years the Pennsylvania State University (PSU) under the sponsorship of the U.S. Nuclear Regulatory Commission (NRC) has prepared, organized, conducted and summarized the OECD/NRC Full-size Fine-mesh Bundle Tests (BFBT) Benchmark. The international benchmark activities have been conducted in cooperation with the Nuclear Energy Agency/Organization for Economic Co-operation and Development (NEA/OECD) and Japan Nuclear Energy Safety (JNES) organization, Japan. Consequently, the JNES has made available the Boiling Water Reactor (BWR) NUPEC database for the purposes of the benchmark. Based on the success of the OECD/NRC BFBT benchmark the JNES has decided to release also the data based on the NUPEC Pressurized Water Reactor (PWR) subchannel and bundle tests for another follow-up international benchmark entitled OECD/NRC PWR Subchannel and Bundle Tests (PSBT) benchmark.

This paper presents an application of the joint Penn State University/Technical University of Madrid (UPM) version of the well-known subchannel code COBRA-TF, namely CTF, to the critical power and departure from nucleate boiling (DNB) exercises of the OECD/NRC BFBT and PSBT benchmarks.

1. Introduction

The increased use and importance of detailed reactor core descriptions for Light Water Reactor (LWR) safety analysis and coupled local neutronics/thermal-hydraulics evaluations requires the use of advanced two-phase thermal-hydraulic codes. These codes must be extensively validated against full-scale high quality experimental data. In that sense, the international OECD/NRC Boiling Water Reactor (BWR) Full-Size Fine-Mesh Bundle Test (BFBT) benchmark [1] and the OECD/NRC PWR Subchannel and Bundle Tests (PSBT) benchmark [2] provide an excellent opportunity for validation of models for critical power and departure from nucleate boiling (DNB).

The OECD/NRC BFBT and PSBT benchmarks were established to provide test beds for assessing the capabilities of various thermal-hydraulic subchannel, system, and computational fluid dynamics (CFD) codes and to encourage advancement in the analysis of fluid flow in rod bundles. The aim was to improve the reliability of the nuclear reactor safety margin evaluations. The benchmarks are based on one of the most valuable databases identified for the thermal-hydraulics modelling, which was developed by the Nuclear Power Engineering Corporation (NUPEC) in Japan.

This paper presents results obtained with the thermal-hydraulic code CTF [3] for the Exercise II-1 (Steady-state critical power) of the OECD/NRC BFBT benchmark and Exercise II-1 (Steady-state departure from nucleate boiling) of the OECD/NRC PSBT benchmark. CTF is a transient code based on a separated flow representation of the two-phase flow. The two-fluid formulation, generally used in thermal-hydraulic codes, separates the conservation equations of mass, energy, and momentum to vapor and liquid. CTF extends this treatment to three fields: vapor, continuous liquid and entrained liquid droplets, which results in a set of nine time-averaged conservation equations. The conservation equations for each of the three fields and for heat transfer from and within the solid structure in contact with the fluid are solved using a semi-implicit, finite-difference numerical technique on an Eulerian mesh, where time intervals are assumed to be long enough to smooth out the random fluctuations in the multiphase flow, but short enough to preserve any gross flow unsteadiness. The code is able to handle both hot wall and normal flow regimes maps and it is capable of calculating reverse flow, counter flow, and crossflow situations. The code is developed for use with either 3D Cartesian or subchannel coordinates and, therefore, the code features extremely flexible nodding for both the thermal-hydraulic and the heat-transfer solution. This flexibility allows a fully 3D treatment in geometries amenable to description in a Cartesian coordinate system.

The code version used in the presented work is being maintained during the last few years by the Reactor Dynamics and Fuel Management Group (RDFMG), the Pennsylvania State University (PSU) in cooperation with the Technical University of Madrid (UPM) in Spain. The original version of COBRA-TF was developed at the Pacific Northwest Laboratory as a part of the COBRA/TRAC thermal-hydraulic code. Since then, various academic and industrial organizations have adapted, developed and modified the code in many directions. The code is worldwide used for academic and general research purposes as well. The code version used at PSU originates from a code version modified during the FLECHT SEASET program [5]. In parallel to the code utilization to teach and train students in the area of nuclear reactor thermal-hydraulic safety analyses at PSU and UPM during the last few years, the theoretical models and numerics of COBRA-TF were substantially improved [6,7,8,9]. The code was subjected to an

extensive verification and validation program and was applied to variety of LWR steady state and transient simulations. CTF is being used at both universities for coupling with different 3D neutron-kinetics codes. At UPM, the code is part of the COBAYA3 [10] system of codes for multiphysics and multiscale core calculations. The code has been coupled with the ANDES nodal scale diffusion code [11] for nodal calculations and with the COBAYA3K pin-by-pin diffusion code [12] for fine mesh calculations. Both systems of coupled codes are part of a multiscale calculation methodology based on a subdomain decomposition of the core for fast pin-by-pin diffusion calculations of the whole core [13]. Validation of this system is being carried out [14]. At PSU, a 3D neutron kinetics module was implemented into CTF by a serial integration coupling to the PSU NEM code. The new PSU coupled code system was named CTF/NEM [15].

2. Brief Description of the CTF Flow Regimes and Heat Transfer Package

The flow regime map used in the CTF can be divided into two main parts: the logic used to select physical models in the absence of unwetted hot surfaces (“normal” flow regimes), and the logic used when hot surfaces are present (“hot wall” flow regimes). Since the code was originally developed for vertical two-phase flow, horizontal flow regimes were not considered; however, an implementation of a horizontal flow regime map is being currently carried out at PSU [16]. The physical models used in the numerical solution must be defined for each mesh cell. Therefore, the flow regime must be determined from fluid properties and flow conditions within each cell or in the immediate surrounding cells. The physical models are selected using the normal flow regime logic if a mesh cell does not contain any solid surface with a temperature greater than $T_{\text{sat}}+75^{\circ}\text{F}$. The flow regimes considered include dispersed bubbly flow, slug flow, churn-turbulent flow, film flow and film mist flow. The “hot wall” flow regimes describe the hydrodynamics of the highly non-homogenous, thermal non-equilibrium, two-phase flow encountered during reflood. These flow regimes include subcooled inverted annular flow, saturated liquid chunk flow, dispersed drop-vapor flow, falling film flow and top deluge.

The heat transfer models in CTF determine the material heat release rates and the temperature response of the fuel rod and structural components of LWR's during operating and transient conditions. All the heat transfer calculations are performed at the beginning of each time step before the hydraulic solution. Heat transfer coefficients based on previous time step liquid conditions are used to advance the material conduction solution. The resultant heat release rates are explicitly coupled to the hydrodynamic solution as source terms in the fluid energy equations.

The CTF heat transfer package consists of a library of heat transfer coefficients and a selection logic algorithm. Together these produce a boiling curve that is used to determine the phasic heat fluxes. The heat transfer regime selection logic and the correlations used in each regime are briefly discussed below:

Single-Phase Vapor: The maximum of the Dittus-Boelter turbulent convection correlation [17], the FLECHT SEASET 161-rod steam cooling correlation [18], and a laminar flow Nusselt number is used. For single-phase convection to vapor, all vapor properties are evaluated at the film temperature.

Single-Phase Liquid: Convection to single-phase liquid is computed as the larger of either the Dittus-Boelter turbulent convection correlation or the laminar flow with a limit Nusselt number equal to 7.86 [19].

Nucleate boiling: When the temperature is greater than saturation but less than the critical heat flux temperature and liquid is present, the Chen nucleate boiling correlation [20] is used. The Chen correlation applies to both the saturated nucleate boiling region and the two-phase forced convection evaporation region. It automatically makes the transition to single-phase convection at low wall superheat and pool boiling at low flow rate. The Chen correlation assumes a superposition of a forced-convection correlation (Dittus-Boelter type) and a pool boiling equation (Forster-Zuber).

Subcooled Nucleate Boiling: An extension of the Chen nucleate boiling correlation into the subcooled region is used for subcooled nucleate boiling. During the subcooled boiling, vapor generation occurs and a significant void fraction may exist despite the presence of subcooled water. The processes of interest in this regime are forced convection to liquid, vapor generation at the wall, condensation near the wall, and bulk condensation (subcooled liquid core).

Critical Heat Flux and Transition Boiling Regime: Three critical heat flux regimes are considered – pool boiling, forced convection DNB, and annular film dryout. Pool boiling DNB is selected when the mass flux is low (below $30 \text{ g/cm}^2\text{-sec}$) and the flow regime is not annular film flow. The pool boiling heat flux is given by Griffith's [21] modification of the Zuber [22] equation. The critical heat flux in this region is chosen as the larger of the Griffith's modification and the forced convection DNB heat flux at a mass flux of $30 \text{ g/cm}^2\text{-sec}$. Forced-convection DNB is considered when the mass flux is greater than $30 \text{ g/cm}^2\text{-sec}$ and the flow regime is not annular film flow. The critical heat flux is given by the Biasi correlation [23], which consists of two equations, one for low-quality CHF and one for high-quality CHF. The critical heat flux is defined as the maximum of the two equations. If annular flow exists, the departure from nucleate boiling is caused by annular film dryout. In this regime, the heat flux is not limited by a correlation, but rather forced convection vaporization exists until the film dries out. Film dryout is a complex function of the film flow rate, the applied heat flux, and the entrainment-de-entrainment rate. Film dryout is determined by the solution of the hydrodynamic equations. A value of $75 \text{ }^\circ\text{F}$ wall superheat is selected to be a CHF point for annular film dryout and the CHF is set to that given by the Zuber equation. The critical heat flux temperature is defined using an iterative procedure to determine the wall temperature at which the heat flux from the Chen nucleate boiling correlation is equal to the CHF.

The transition boiling regime is bounded by the CHF point (below which the wall is continuously wetted and nucleate boiling exists) and the minimum stable film boiling point (above which the liquid cannot wet the wall and film boiling exists). It is assumed that the minimum film boiling temperature is the wall temperature that results in an instantaneous contact temperature equal to the homogeneous nucleation temperature. In addition, the minimum film boiling temperature is restricted to varies between $800 \text{ }^\circ\text{F}$ and $1200 \text{ }^\circ\text{F}$.

CTF employs a simple additive scheme for heat transfer beyond the critical heat flux temperature. It is assumed that the transition boiling heat transfer is composed of both liquid contact (wet wall) and film boiling (dry wall).

Dispersed flow film boiling: Heat transfer in the film boiling region is assumed to result either from dispersed flow film boiling or from inverted annular film boiling.

Dispersed flow film boiling is selected if the void fraction is greater than 0.8. It is treated by a “two-step” method where the dominant heat transfer mode is forced convection to superheated steam. The steam superheat is determined by the interfacial heat transfer rate to the entrained droplets as part of the hydrodynamic solution. Heat fluxes due to wall-droplet radiation and droplet impingement are superimposed upon the vapor convective heat flux.

Inverted Annular Film Boiling: When the void fraction is less than 0.6, inverted annular film boiling is assumed to occur. The heat flux for this regime is computed from the larger of either dispersed film boiling heat flux as defined above, or the value from the modified Bromley correlation [24]. At intermediate void fractions ($0.8 > \alpha > 0.6$), the heat flux is interpolated between the value for inverted annular and dispersed flow film boiling.

3. CTF Application to the Steady State Critical Power Exercise of the OECD/NRC BWR Full-size Fine-mesh Bundle Tests Benchmark

From 1987 to 1995, NUPEC performed a series of void measurement tests using full-size mock-up tests for both BWRs and PWRs. Based on state-of-the-art computer tomography (CT) technology, the void distribution was visualized at the mesh size smaller than the subchannel under actual plant conditions. NUPEC also performed steady state and transient critical power test series based on the equivalent full-size mock-ups. Considering the reliability not only of the measured data, but also other relevant parameters such as the system pressure, inlet sub-cooling and rod surface temperature, these test series supply the first substantial database for the development of truly mechanistic and consistent models for void distribution and boiling transition.

The full scale test bundle, simulating an 8×8 high burn-up fuel assembly, was installed in the test section. Three combinations of radial and axial power shapes were tested: 1) beginning of cycle (BOC) radial power pattern/cosine axial power shape; 2) end of cycle (EOC) radial power pattern/cosine axial power shape; and 3) beginning of cycle radial power pattern/inlet peaked axial power shape. The individual radial and axial power distributions for all three combinations are provided in Volume I of the BFBT benchmark specifications [1].

The steady-state test series consisted of two parts: pressure drop measurements and critical power tests. The pressure drop was measured in both single-phase flow and two-phase flow conditions that cover the normal operational behavior. CTF has been previously applied to the single- and two-phase pressure drop cases of the BFBT benchmark and has shown excellent agreement with the single-phase pressure drop data and slight over-prediction of the two-phase pressure drop data due to overestimated interfacial drag forces [25].

The critical power was measured by slowly increasing the bundle power while monitoring the individual heater rod thermocouple signals. The critical power was defined when the peak rod surface temperature became 14°C higher than the steady-state temperature level before dry-out occurred. The dry-out was observed in the peak power rod located at the peripheral row adjacent

to the channel box. The boiling transition was always observed just upstream of the spacer. The estimated accuracies of the major process parameters were 1% and 1.5% for the pressure and power, respectively. Figure 1 describes the definition of thermocouple position. Each thermocouple position was identified as follows: *Rod No. – Axial location – Rotational angle*.

Assembly C2A exercise cases were simulated in this work. The supplied measured data includes critical power, axial location of boiling transition and corresponding boundary conditions (pressure, flow, inlet sub-cooling and power shapes). The radial and axial power profiles of assembly type C2A are given in Table I.

A full C2A bundle model on a subchannel-by subchannel special resolution - no symmetry - was used in the CTF calculations. The heated length was divided axially into forty (40) equidistant nodes. The pressure losses due to spacer grids were calculated as velocity head losses with subchannel loss coefficient as calculated by the Shiralkar's method [25]. The total cross-flow between two adjacent subchannels was simulated as a sum of the diversion cross-flow due to lateral pressure gradients and the lateral flow due to turbulent mixing and void drift. Turbulent mixing and void drift phenomena are modeled in CTF by the Lahey & Moody approach [26], where the net two-phase mixing (including void drift) is assumed to be proportional to the non-equilibrium void fraction gradient. The void drift is only assumed to occur in bubbly, slug, and churn flow, where liquid is the continuous phase and vapor is the dispersed phase. The single phase mixing coefficient might be either specified as an input value or calculated using an empirical correlation derived by Rogers and Rosehart [27]. The Beus' model for two-phase turbulent mixing is utilized [28].

A sensitivity study was performed on the three different turbulent mixing options available in the code: (1) no turbulent mixing, (2) Lahey & Moody model with a user-specified single-phase mixing coefficient, and (3) Lahey & Moody model with a single-phase mixing coefficient by Rogers and Rosehart's correlation and Beus' model for two-phase mixing enhancement.

In the CTF calculations, the bundle power was increased until the peak rod surface temperature became 14°C higher than the temperature at the previous steady-state level.

Results are summarized in Figures 2, 3, 4, and 5. As it can be seen, the best agreement is obtained when no crossflow by turbulent mixing and void drift was modeled. The mean relative error in the code predictions was found to be 3.4%. Including lateral exchange of momentum, mass, and heat due to increased turbulence in the flow had an adverse effect on the code accuracy of dryout prediction resulting in an overestimation of the critical power. Stronger was the turbulent mixing larger was the overprediction (for typical BWR bundles, Rogers and Rosehart correlation generally gives a single-phase mixing coefficient in the order of 10E-3). This result was to be expected for the C2A type bundle – the spacers instrumented along the bundle are ferrule type spacers which are not designed to enhance the turbulence of the flow. On another hand, in the CTF simulations, the lateral pressure gradient due to spacers was accounted for by applying subchannel-based loss coefficients in both axial and transverse direction. Crossflow due to coolant temperature and density gradients is handled by the diversion crossflow models.

Another observation in the code predictions was the bias with the pressure – the code tends to overpredict the critical power at lower pressure (~ 5.5 MPa) and to underpredict it at higher pressure (~ 9 MPa). No bias was seen with the flow rate and the subcooling.

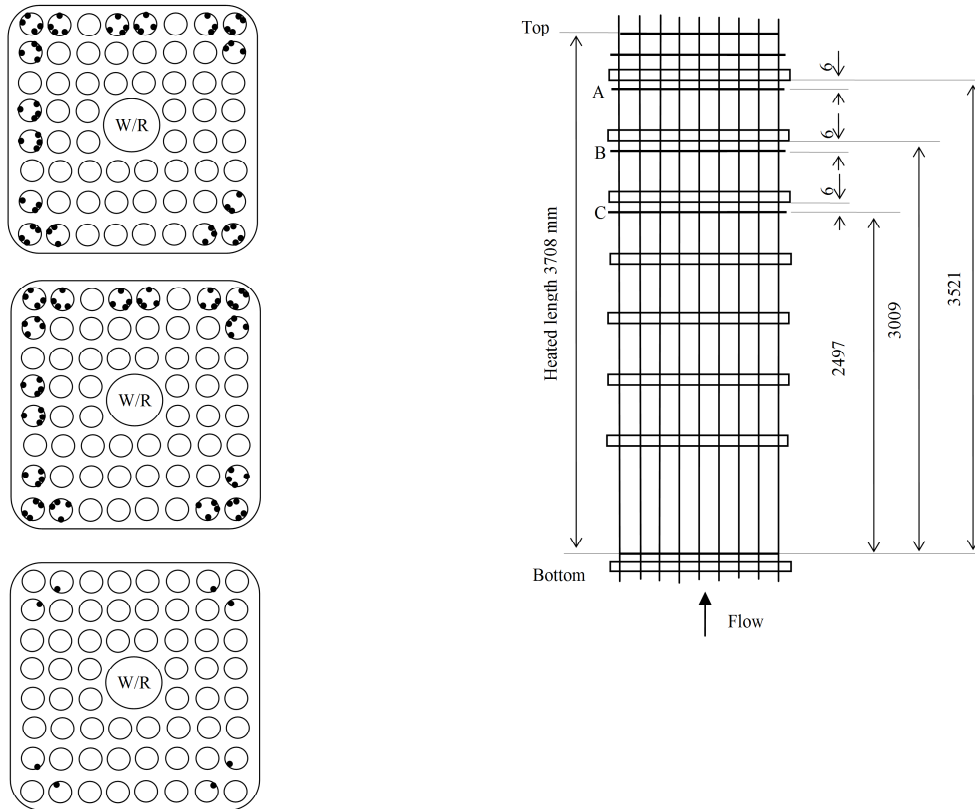
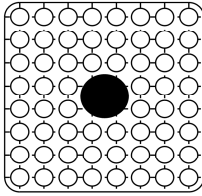
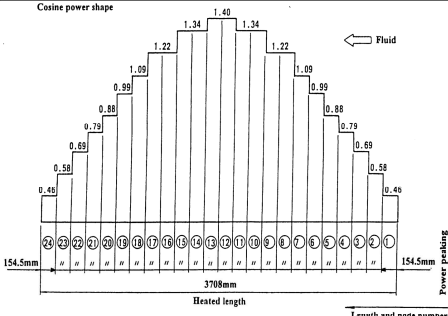


Figure 1. Definition of Thermocouple Position for Assembly C2A [1]

Table I. Steady-State Critical Power Measurement Conditions for Assembly C2A [1]

 <p>C2A</p>	 <p>Axial power profile</p>		<table border="1" data-bbox="925 1545 1292 1758"> <tr><td>1.15</td><td>1.30</td><td>1.15</td><td>1.30</td><td>1.30</td><td>1.15</td><td>1.30</td><td>1.15</td></tr> <tr><td>1.30</td><td>0.45</td><td>0.89</td><td>0.89</td><td>0.89</td><td>0.45</td><td>1.15</td><td>1.30</td></tr> <tr><td>1.15</td><td>0.89</td><td>0.89</td><td>0.89</td><td>0.89</td><td>0.89</td><td>0.45</td><td>1.15</td></tr> <tr><td>1.30</td><td>0.89</td><td>0.89</td><td></td><td></td><td>0.89</td><td>0.89</td><td>1.15</td></tr> <tr><td>1.30</td><td>0.89</td><td>0.89</td><td></td><td></td><td>0.89</td><td>0.89</td><td>1.15</td></tr> <tr><td>1.15</td><td>0.45</td><td>0.89</td><td>0.89</td><td>0.89</td><td>0.89</td><td>0.45</td><td>1.15</td></tr> <tr><td>1.30</td><td>1.15</td><td>0.45</td><td>0.89</td><td>0.89</td><td>0.45</td><td>1.15</td><td>1.30</td></tr> <tr><td>1.15</td><td>1.30</td><td>1.15</td><td>1.15</td><td>1.15</td><td>1.15</td><td>1.30</td><td>1.15</td></tr> </table> <p>Radial Power Profile</p>		1.15	1.30	1.15	1.30	1.30	1.15	1.30	1.15	1.30	0.45	0.89	0.89	0.89	0.45	1.15	1.30	1.15	0.89	0.89	0.89	0.89	0.89	0.45	1.15	1.30	0.89	0.89			0.89	0.89	1.15	1.30	0.89	0.89			0.89	0.89	1.15	1.15	0.45	0.89	0.89	0.89	0.89	0.45	1.15	1.30	1.15	0.45	0.89	0.89	0.45	1.15	1.30	1.15	1.30	1.15	1.15	1.15	1.15	1.30	1.15
	1.15	1.30	1.15	1.30	1.30	1.15	1.30	1.15																																																												
1.30	0.45	0.89	0.89	0.89	0.45	1.15	1.30																																																													
1.15	0.89	0.89	0.89	0.89	0.89	0.45	1.15																																																													
1.30	0.89	0.89			0.89	0.89	1.15																																																													
1.30	0.89	0.89			0.89	0.89	1.15																																																													
1.15	0.45	0.89	0.89	0.89	0.89	0.45	1.15																																																													
1.30	1.15	0.45	0.89	0.89	0.45	1.15	1.30																																																													
1.15	1.30	1.15	1.15	1.15	1.15	1.30	1.15																																																													
Boundary Conditions	Pressure (MPa) Flow rate (t/h) Inlet Subcooling (KJ/kg)	5.5, 7.2, 8.6 10, 20, 30, 45, 55, 60, 65 25, 50, 84, 104, 126																																																																		
No. of Cases	Exercise cases	14																																																																		

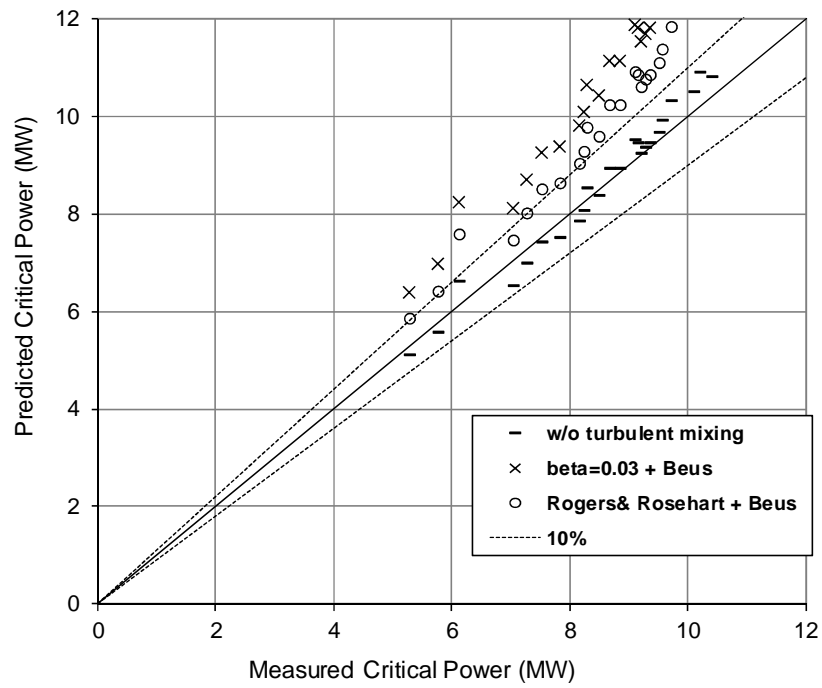


Figure 2. Predicted versus Measured Critical Power for Assembly C2A with Different Turbulent Mixing Models

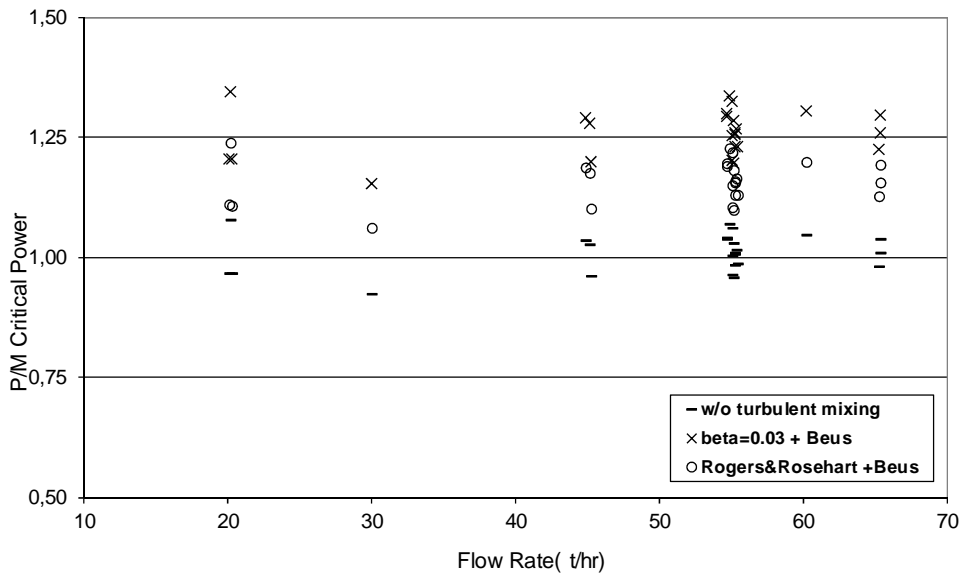


Figure 3. P/M Critical Power versus Flow Rate for Assembly Type C2A

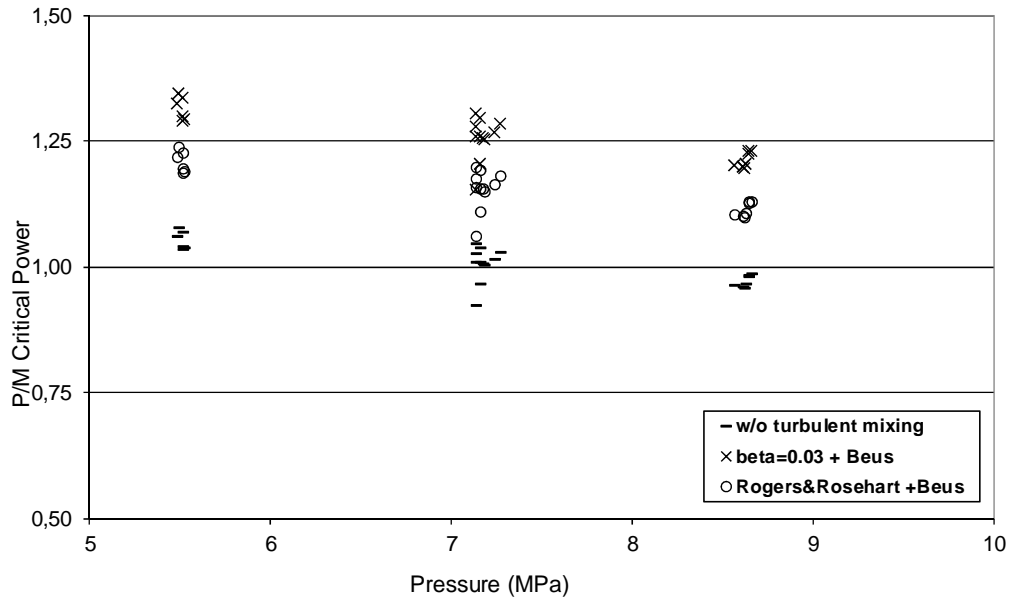


Figure 4. P/M Critical Power versus Pressure for Assembly Type C2A

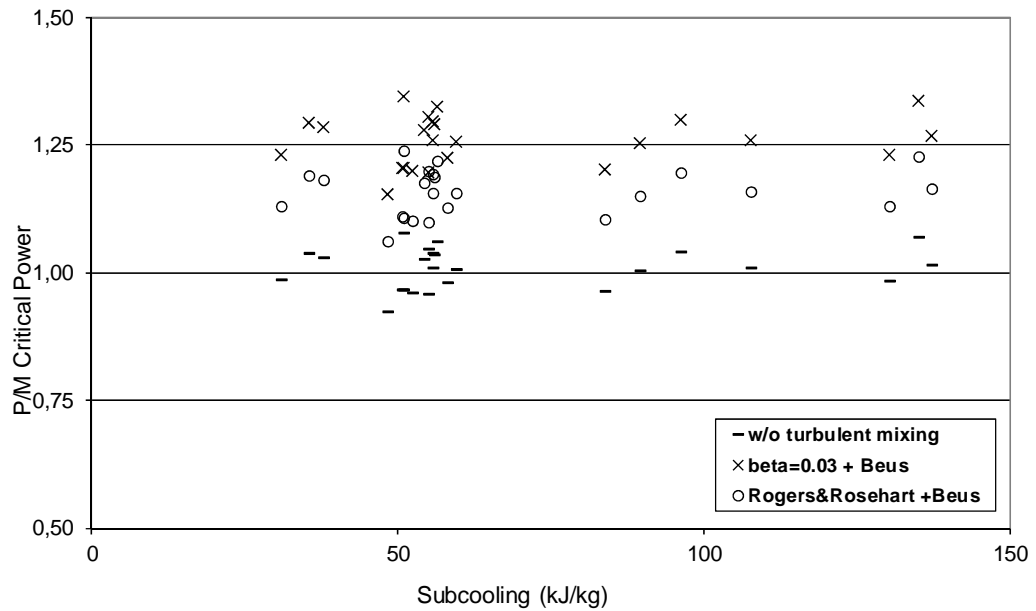


Figure 5. P/M Critical Power versus Subcooling for Assembly Type C2A

4. CTF Application to the Steady State DNB Exercise of the OECD/NRC PWR Subchannel and Bundle Tests Benchmark

In the NUPEC PWR DNB measurements, the test assembly configuration nominally consisted of twenty-five rods in a 5×5 square bundle [2]. The configuration of rods in this geometry approximates a typical 17×17 commercial power reactor fuel assembly. Each rod has a heated length of 3.658m, an outer diameter of 9.5mm, and a rod pitch of 12.6mm. Approximately 15 spacers (both with and without mixing vanes) along the axial length support the rods in the vertical grid. The rods are cylindrical in shape with a hollow insulator of alumina radially encircled in a heater made from Inconel 600. For the steady-state departure from nucleate boiling case considered in this paper, a series of experiments were performed in five different configurations [2]. The NUPEC test series (numbered 0, 2, 3, 4, 8, and 13) were conducted at various pressures and temperatures where prior experience demonstrated that departure from nucleate boiling was likely to occur. The thermocouples were attached to the inner surface of the heater rods to determine the boiling transition. The bundle power was increased gradually by fine steps to the vicinity of DNB power, which was based on preliminary analysis. The occurrence of DNB was confirmed by a rod temperature rise of more than 11°C as measured by the thermocouples. The DNB power was defined as the power corresponding to the step just before the step where the temperature increased. Figure 6 shows the axial position of the thermocouples for each configuration. The various test configurations used several axial and radial power schemes, which provided an ample cross-section of calculation data. Five assemblies were utilized; denoted as A0, A2, A3, A4, and A8 (see Table II and Table III). The estimated accuracies of different process parameters for the DNB measurements were: pressure - 1%; flow - 1.5%; fluid temperature - 1°C; and power - 1%.

Approximately, twenty-five data points consisting of pressure temperature and DNB location were chosen from configurations A4 (Test Series 4 and 13) and A8 (Test Series 8) as good candidates for the benchmark test. An additional ten were chosen from each of the remaining test series (Test Series 0, 2, and 3). From all test sources, one hundred data points were modeled by the CTF code.

The default models, described in Section 2, for the flow regimes and heat transfer modes transition were utilized in these CTF simulations. The calculations were performed in two sets: (1) without modelling of turbulent mixing and void drift; and (2) turbulent mixing and void drift by Lahey & Moody with a user-specified single-phase mixing coefficient of 0.05 and Beus' model for two-phase mixing enhancement.

The PSBT bundles were equipped with three different spacer types: single support spacer, non-mixing vane spacers, and mixing vane spacers [2]. While the first two types mostly affect the pressure drop in the bundles, the third type spacers increase the turbulence of the flow and create strong crossflows between the subchannels. And therefore, as it can be seen in Figures 7 and 8, the agreement is significantly improved when turbulent mixing and void drift are modelled: a large underprediction on the DNB power with a mean relative error of 17% if no mixing versus a mean relative error of 8 % if mixing is included.

Similarly to the BFBT critical power calculations, a code bias with the pressure was seen (Figure 9) – the code tends to overpredict the critical power at lower pressure (~ 5 MPa) and to

underpredict it at higher pressure (~ 15 MPa). No bias with the flow rate and the subcooling was found (Figures 10 and 11).

5. Conclusions

To validate its accuracy of dryout and critical heat flux calculations, the subchannel thermal-hydraulic code CTF was applied to Exercise II-1 (steady-state critical power) of the OECD/NRC BFBT benchmark and Exercise II-1 (steady-state departure from nucleate boiling) of the OECD/NRC PSBT benchmark. The obtained results have shown that the code predicts fairly well the critical power and departure from nucleate boiling power with no specific tendency of over- or underprediction. However, a clear bias with the pressure was found in the code simulations. In conclusion, further improvements of the CTF logic for flow regime transition and heat transfer modes are needed.

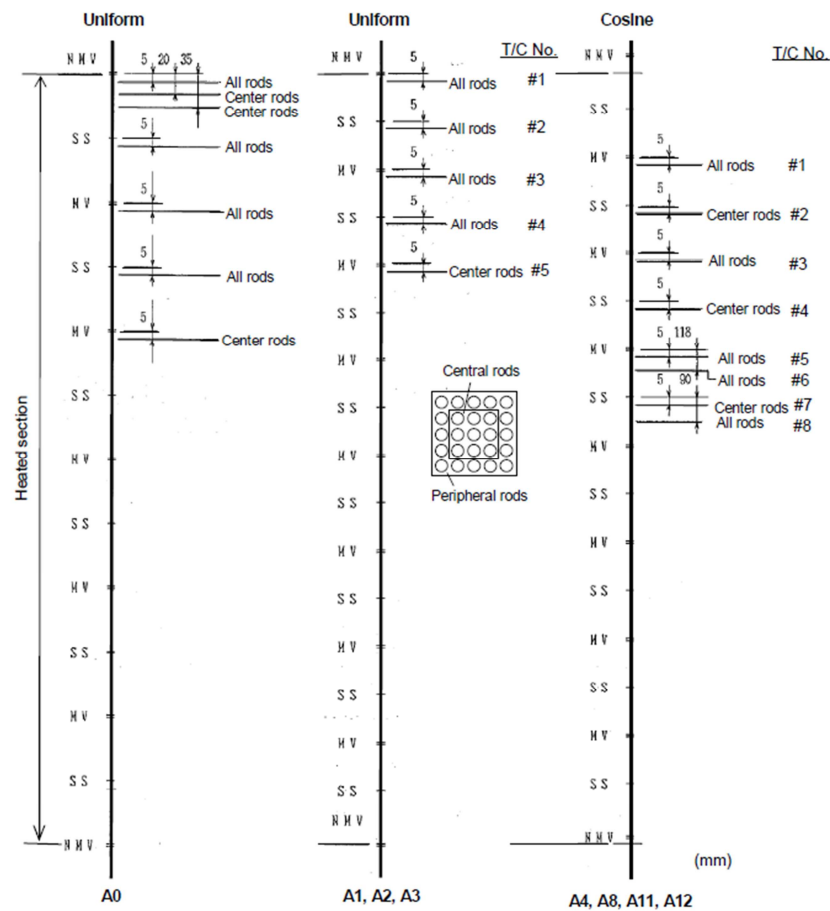


Figure 6. Axial Thermocouple Locations in the PSBT DNB Measurements [2]

Table II. Geometry and Power Shape for Test Assembly A0, A2, and A3 [2]

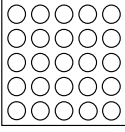
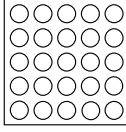
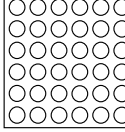
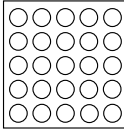
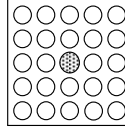
Item	Data		
Assembly			
	A0	A2	A3
Rods array	5×5	5×5	6×6
Number of heated rods	25	25	36
Number of thimble rods	0	0	0
Heated rod outer diameter (mm)	9.50	9.50	9.50
Thimble rod outer diameter (mm)	-	-	-
Heated rods pitch (mm)	12.60	12.60	12.60
Axial heated length (mm)	3658	3658	3658
Flow channel inner width (mm)	64.9	64.9	77.5
Radial power shape	A	A	D
Axial power shape	Uniform	Uniform	Uniform
Number of MV spacers	7	7	7
Number of NMV spacer	2	2	2
Number of simple spacers	8	8	8
MV spacer location (mm)	457, 914, 1372, 1829, 2286, 2743, 3200		
NMV spacer location (mm)	0, 3658		
Simple spacer location (mm)	229, 686, 1143, 1600, 2057, 2515, 2972, 3429		

Table III. Geometry and Power Shape for Test Assembly A4 and A8 [2]

Item	Data	
Assembly		
	A4	A8
Rods array	5×5	5×5
Number of heated rods	25	24
Number of thimble rods	0	1
Heated rod outer diameter (mm)	9.50	9.50
Thimble rod outer diameter (mm)	-	12.24
Heated rods pitch (mm)	12.60	12.60
Axial heated length (mm)	3658	3658
Flow channel inner width (mm)	64.9	64.9
Radial power shape	A	B
Axial power shape	Cosine	Cosine
Number of MV spacers	7	7
Number of NMV spacer	2	2
Number of simple spacers	8	8
MV spacer location (mm)	471, 925, 1378, 1832, 2285, 2739, 3247	
NMV spacer location (mm)	2.5, 3755	
Simple spacer location (mm)	237, 698, 1151, 1605, 2059, 2512, 2993, 3501	

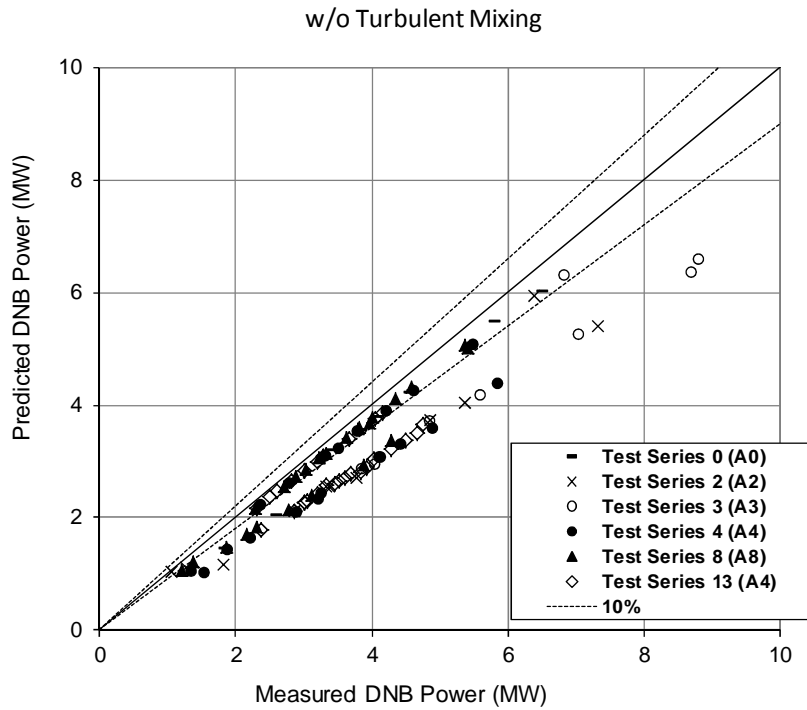


Figure 7. Axial Thermocouple Locations in the PSBT DNB Measurements

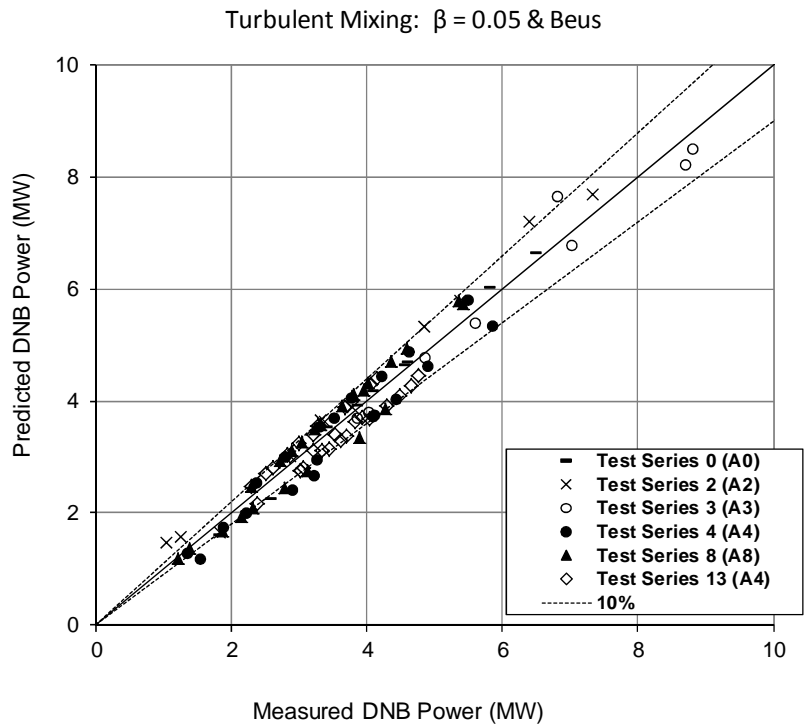


Figure 8. Axial Thermocouple Locations in the PSBT DNB Measurements

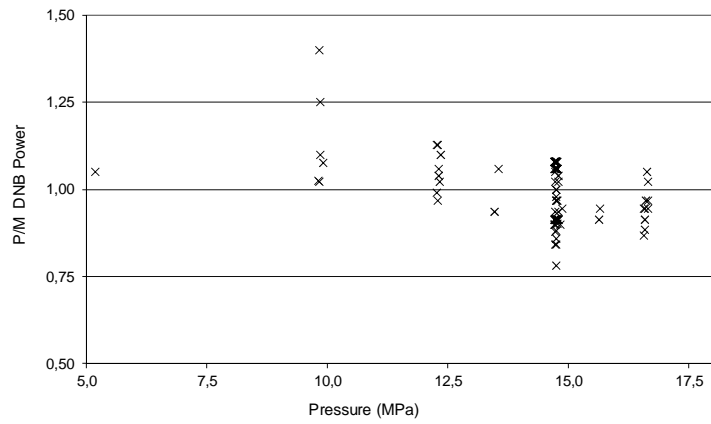


Figure 9. P/M DNB Power versus Pressure for Assembly Types A0, A2, A3, A4, and A8

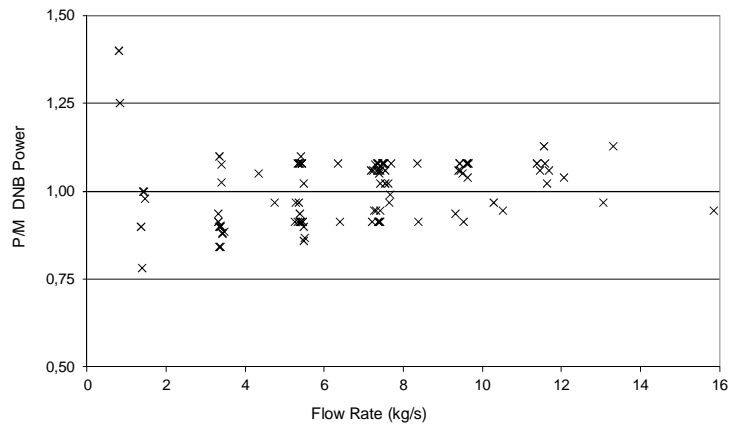


Figure 10. P/M DNB Power versus Flow Rate for Assembly Types A0, A2, A3, A4, and A8

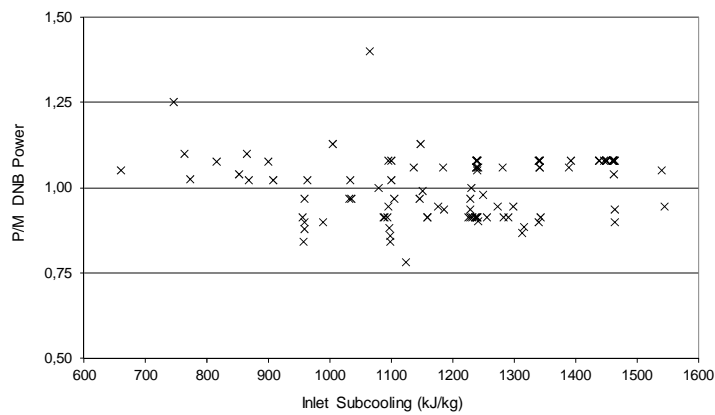


Figure 11. P/M DNB Power versus Subcooling for Assembly Types A0, A2, A3, A4, and A8

8. References

- [1] B. Neykov, et al., "OECD-NEA/US-NRC/NUPEC BWR Full-size Fine-mesh Bundle Test (BFBT) Benchmark, Volume I: Specifications", OECD 2006, NEA No. 6212, NEA/NSC/DOC(2005)5, ISBN 92-64-01088-2 (2006)
- [2] A. Rubin, et al., "OECD/NRC Benchmark Based on NUPEC PWR Subchannel and Bundle Tests (PSBT). Volume I: Experimental Database and Final Problem Specifications", NEA/NSC/DOC(2010)1, January 2010
- [3] "CTF - A Thermal-Hydraulic Subchannel Code for LWRs Transient Analyses. User's Manual", Technical Report, RDFMG, The Pennsylvania State University, December 2004
- [4] M.J. Thurgood, et al., "COBRA/TRAC – A Thermal-Hydraulic Code for Transient Analysis of Nuclear Reactor Vessel and Primary Coolant Systems", NUREG/CR-3046 (1983)
- [5] C. Y. Payk et al., Analysis of FLECHT SEASET 163-Rod Blocked Bundle Data using COBRA-TF, NRC/EPRI/Westinghouse-12, (1985).
- [6] M. Avramova, "COBRA-TF Development, Qualification, and Application to LWR Analysis", MS Thesis, The Pennsylvania State University (2003)
- [7] D. Cuervo, et al., "Evaluation and Enhancement of COBRA-TF Efficiency for LWR Calculations", Annals of Nuclear Energy (2006)
- [8] M. Avramova, et al., "Improvements and Applications of COBRA-TF for Stand-Alone and Coupled LWR Safety Analyses", Proceedings: PHYSOR-2006, Vancouver, Canada, September 2006
- [9] M. Avramova, "Development of an Innovative Spacer Grid Model Utilizing Computational Fluid Dynamics within a Subchannel Analysis Tool", PhD Thesis, The Pennsylvania State University (2007)
- [10] J.J. Herrero, J. Jimenez, J.A. Lozano, N. García-Herranz, C. Ahnert, J.M. Aragonés, "The 3D Cell-Nodal Multi-scale COBAYA3 Code", NURESIM Deliverable D1.2.3, Department of Nuclear Engineering, Technical University of Madrid (UPM), 2008
- [11] J. Lozano, J.M. Aragonés, N. García-Herranz, "The analytic nodal diffusion solver ANDES in multigroups for 3D rectangular geometry: Development and performance analysis", Annals of Nuclear Energy, 2008, 35, 2365-2374
- [12] J.J. Herrero, C. Ahnert, J.M. Aragonés, "3D Whole Core Fine Mesh Multigroup diffusion calculations by Domain Decomposition through Alternate Dissections", Proceedings: M&C/SNA-2007, Monterey, California (2007)
- [13] J. Jiménez, D. Cuervo, J.M. Aragonés, "A domain decomposition methodology for pin by pin coupled neutronic and thermal-hydraulic analyses in COBAYA3", Nuclear Engineering and Design 240 (2010) 313-320
- [14] J. Jiménez, "Desarrollo e implementación de la descomposición en subdominios mediante disecciones alternadas al acoplamiento neutrónico-termohidráulico en PWR con un sistema de cálculo multiescala", PhD Thesis, Technical University of Madrid (2010)

- [15] RDFMG, Nuclear Engineering Program, “CTF/NEM – A Coupled Neutronics/Thermal-Hydraulic Code for LWRs Transient Analyses, Users’ Manual”, University Park, PA, 2007
- [16] R. K. Salko, M. Avramova, A. Ohnuki, "Modification of COBRA-TF for Improved Vessel-Wide Transient Analysis", 2010 ANS Winter Meeting, Las Vegas, Nevada, USA, November 2010, Vol. 103, pp. 977-978
- [17] F.W. Dittus, and L.M.K. Boelter, “Heat Transfer in Automobile Radiators of Tubular Type”, University of California, Berkeley Publ. Eng. 2,13, 1930, 442-462
- [18] S.Wong and L.E. Hochreiter, “Analysis of the FLECHT SEASET Unblocked Bundle Steam Cooling and Boiloff Tests’, NRC/EPRI/Westinghouse-8, January 1981
- [19] E.M. Sparrow, et al., “Heat Transfer to Longitudinal Laminar Flow Between Cylinders”, Journal of Heat Transfer 83, 415, 1961
- [20] J.C. Chen, “A Correlation for Boiling Heat Transfer to Saturated Fluids in Convective Flow”, ASME 63-HT-34, American Society of Mechanical Engineers, 1963
- [21] P. Griffith, et al., “PWR Blowdown Heat Transfer”, Thermal and Hydraulic Aspects of Nuclear Reactor Safety, American Society of Mechanical Engineers, New York, Vol.1, 17-41, 1977
- [22] N. Zuber, et al, “The Hydraulics Crisis in Pool Boiling of Saturated and Subcooled Liquids”, Part II, No.27, 23-236 in International Developments in Heat Transfer, International Heat Transfer Conference, Boulder, Colorado, 1961
- [23] L. Biasi, et al., “Studies on Burnout, Part 3”, Energia Nucleate, 14(9), 530-536, 1967
- [24] L.A. Bromley, “Heat Transfer in Stable Film Boiling”, Chemical Engineering Progress 46(5), 221-226, 1950
- [25] M. Avramova, et al., “Analysis of Void Distribution Predictions for Phase I of the OECD/NRC BFBT Benchmark using CTF/NEM”, Proceedings: NURETH-12, Pittsburgh, Pennsylvania, USA, September 2007
- [26] R. T. Lahey and F. J. Moody, The Thermal Hydraulics of a Boiling Water Nuclear Reactor, American Nuclear Society (ANS) (1993)
- [27] J. T. Rogers and R. G. Rosehart, Mixing by Turbulent Interchange in Fuel Bundles, Correlations and Inferences, ASME, 72-HT-53,(1972)
- [28] S. G. Beus, A two-phase turbulent mixing model for flow in rod bundles. Bettis Atomic Power Laboratory, WAPD-T-2438, (1970)